

# Electroweak chiral Lagrangians and the Higgs properties at the one-loop level

J.J. Sanz-Cillero<sup>1,a</sup>

<sup>1</sup>*Departamento de Física Teórica and Instituto de Física Teórica, IFT-UAM/CSIC  
 Universidad Autónoma de Madrid, C/ Nicolás Cabrera 13-15,  
 Cantoblanco, 28049 Madrid, Spain*

**Abstract.** In these proceedings we explore the use of (non-linear) electroweak chiral Lagrangians for the description of possible beyond the Standard Model (BSM) strong dynamics in the electroweak (EW) sector. Experimentally one observes an approximate EW symmetry breaking pattern  $SU(2)_L \times SU(2)_R / SU(2)_{L+R}$ . Quantum Chromodynamics (QCD) shows a similar chiral structure [1] and, in spite of the differences (in the EW theory  $SU(2)_L \times U(1)_Y$  is gauged), it has served for years as a guide for this type of studies [2–4]. Examples of one-loop computations in the low-energy effective theory and the theory including the first vector (V) and axial-vector (A) resonances are provided, yielding, respectively, predictions for  $\gamma\gamma \rightarrow Z_L Z_L, W_L^+ W_L^-$  and the oblique parameters  $S$  and  $T$ .

## 1 Introduction: strong dynamics and chiral Lagrangians

A non-linear realization of the EW would-be Goldstone bosons (WBGBs) is considered to build the EW low-energy effective field theory (EFT), which is described by an EW chiral Lagrangian with a light Higgs (ECLh). It includes the Standard Model (SM) content: the EW Goldstones  $w^a$ , the EW gauge bosons  $W_\mu^a$  and  $B_\mu$  and a singlet Higgs  $h$  (the fermion sector is not discussed here). In particular, in Sec. 2 we explain the chiral counting in the ECLh [5, 6] and provide an example of a next-to-leading order (NLO) computation: we calculate  $\gamma\gamma \rightarrow W_L^+ W_L^-, Z_L Z_L$  within this framework up to the one-loop level [5] at energies below new possible composite resonances,  $\sqrt{s} \ll \Lambda_{\text{ECLh}} \sim \min\{M_R, 4\pi v\}$  (with  $v = (\sqrt{2}G_F)^{-1/2}$  and  $4\pi v \simeq 3$  TeV). Analogous works on  $WW$ -scattering can be found in Refs. [7].

However, in the case of having heavy composite resonance, the EFT stops being valid when the energy becomes of the order of their masses (expected to be of the order of  $M_R \sim 4\pi v \sim 3$  TeV). One has to introduce these new degrees of freedom in our EW Lagrangian following a procedure analogous to that in QCD [8]. Likewise, under reasonable ultraviolet (UV) completion hypotheses like, e.g., the Weinberg sum-rules (WSRs) fulfilled by certain types of theories [9–13], one can make predictions on low-energy observables. In Sec. 3 we write down the relevant  $SU(2)_L \times SU(2)_R$  invariant Lagrangian including the SM content and a multiplet of V and A resonances and extract one-loop limits on the resonance masses and the Higgs coupling  $g_{hWW}$  [14] from the experimental values of oblique parameters  $S$  and  $T$  [15]. Alternative one-loop analyses can be found in Refs. [10, 16].

<sup>a</sup>e-mail: [juan.j.sanz@uam.es](mailto:juan.j.sanz@uam.es)

I would like to thank the organizers for their work and the lively discussion during the workshop; also for their patience. This work is partially supported by the Spanish Government and ERDF funds from the European Commission [FPA2010-17747, FPA2013-44773-P, SEV-2012-0249, CSD2007-00042] and the Comunidad de Madrid [HEPHACOS S2009/ESP-1473].

## 2 Low-energy EFT: ECLh and one-loop $\gamma\gamma \rightarrow W_L^a W_L^b$ scattering

The Higgs boson does not enter in the SM at tree-level in these processes (where one also has  $\mathcal{M}(\gamma\gamma \rightarrow ZZ)_{\text{SM}}^{\text{tree}} = 0$ ). Nevertheless, one can search for new physics by studying the one-loop corrections [5], which are sensitive to deviations from the SM in the Higgs boson couplings. Our analysis [5] is performed in the Landau gauge and making use of the Equivalence Theorem (Eq.Th.) [17],

$$\mathcal{M}(\gamma\gamma \rightarrow W_L^a W_L^b) \simeq -\mathcal{M}(\gamma\gamma \rightarrow w^a w^b), \quad (1)$$

valid in the energy regime  $m_W^2, m_Z^2 \ll s$ . The EW gauge boson masses  $m_{W,Z}$  are then neglected in our computation. Furthermore, since  $m_h \sim m_{W,Z} \ll 4\pi v \simeq 3 \text{ TeV}$  we also neglect  $m_h$  in our calculation. In summary, the applicability range in [5] is

$$m_W^2, m_Z^2, m_h^2 \stackrel{\text{Eq.Th.}}{\ll} s, t, u \stackrel{\text{EFT}}{\ll} \Lambda_{\text{ECLh}}^2, \quad (2)$$

with the upper limit given by the EFT cut-off  $\Lambda_{\text{ECLh}}$ , expected to be of the order of  $4\pi v \simeq 3 \text{ TeV}$  or the mass of possible heavy BSM particles.

The WBGBs are described by a matrix field  $U$  that takes values in the  $SU(2)_L \times SU(2)_R / SU(2)_{L+R}$  coset, and transforms as  $U \rightarrow LUR^\dagger$  [2, 3]. The relevant ECLh with the basic building blocks is

$$U = u^2 = 1 + iw^a \tau^a / v + \mathcal{O}(w^2), \quad D_\mu U = \partial_\mu U + i\hat{W}_\mu U - iU \hat{B}_\mu, \quad V_\mu = (D_\mu U)U^\dagger, \quad u^\mu = -iu^\dagger D^\mu U u^\dagger, \\ \hat{W}_{\mu\nu} = \partial_\mu \hat{W}_\nu - \partial_\nu \hat{W}_\mu + i[\hat{W}_\mu, \hat{W}_\nu], \quad \hat{B}_{\mu\nu} = \partial_\mu \hat{B}_\nu - \partial_\nu \hat{B}_\mu, \quad \hat{W}_\mu = gW_\mu^a \tau^a / 2, \quad \hat{B}_\mu = g' B_\mu \tau^3 / 2, \quad (3)$$

with well-defined transformation properties [3, 5, 14]. Two particular parametrizations of the unitary matrix  $U$  (exponential and spherical) were considered in [5], both leading to the same predictions for the physical (on-shell) observables.<sup>1</sup> We consider the counting  $\partial_\mu, m_W, m_Z, m_h \sim \mathcal{O}(p)$ ,  $D_\mu U, V_\mu \sim \mathcal{O}(p)$  and  $\hat{W}_{\mu\nu}, \hat{B}_{\mu\nu} \sim \mathcal{O}(p^2)$  [5, 6]. We require the ECLh Lagrangian to be CP invariant, Lorentz invariant and  $SU(2)_L \times U(1)_Y$  gauge invariant. Here we focus ourselves on the relevant terms for  $\gamma\gamma \rightarrow w^a w^b$  at leading order (LO)  $-\mathcal{O}(p^2)$ – and NLO in the chiral counting  $-\mathcal{O}(p^4)$ – [3, 5]:

$$\mathcal{L}_2 = -\frac{1}{2g^2} \langle \hat{W}_{\mu\nu} \hat{W}^{\mu\nu} \rangle - \frac{1}{2g'^2} \langle \hat{B}_{\mu\nu} \hat{B}^{\mu\nu} \rangle + \frac{v^2}{4} \left[ 1 + 2a \frac{h}{v} + b \frac{h^2}{v^2} \right] \langle D^\mu U^\dagger D_\mu U \rangle + \frac{1}{2} \partial^\mu h \partial_\mu h + \dots, \quad (4)$$

$$\mathcal{L}_4 = a_1 \text{Tr}(U \hat{B}_{\mu\nu} U^\dagger \hat{W}^{\mu\nu}) + ia_2 \text{Tr}(U \hat{B}_{\mu\nu} U^\dagger [V^\mu, V^\nu]) - ia_3 \text{Tr}(\hat{W}_{\mu\nu} [V^\mu, V^\nu]) - \frac{c_\gamma}{2} \frac{h}{v} e^2 A_{\mu\nu} A^{\mu\nu} + \dots$$

where  $\langle X \rangle$  stands for the trace of the  $2 \times 2$  matrix  $X$ , one has the photon field strength  $A_{\mu\nu} = \partial_\mu A_\nu - \partial_\nu A_\mu$  and the dots stand for operators not relevant within our approximations for  $\gamma\gamma$ -scattering [5].

The amplitudes  $\mathcal{M}(\gamma(k_1, \epsilon_1)\gamma(k_2, \epsilon_2) \rightarrow w^a(p_1)w^b(p_2))$ , with  $w^a w^b = zz, w^+ w^-$ , have the structure

$$\mathcal{M} = ie^2 (\epsilon_1^\mu \epsilon_2^\nu T_{\mu\nu}^{(1)}) A(s, t, u) + ie^2 (\epsilon_1^\mu \epsilon_2^\nu T_{\mu\nu}^{(2)}) B(s, t, u), \quad (5)$$

written in terms of the two independent Lorentz structures  $T_{\mu\nu}^{(1,2)} \sim \mathcal{O}(p^2)$  involving the external momenta, which can be found in [5]. The Mandelstam variables are defined as  $s = (p_1 + p_2)^2$ ,  $t = (k_1 - p_1)^2$  and  $u = (k_1 - p_2)^2$  and the  $\epsilon_i$ 's are the polarization vectors of the external photons.

In dimensional regularization, our NLO computation of the  $\mathcal{M}(\gamma\gamma \rightarrow w^a w^b)$  amplitudes can be systematically sorted out in the form [5]

$$\mathcal{M} = \mathcal{M}_{\text{LO}} + \mathcal{M}_{\text{NLO}} \sim \underbrace{\mathcal{O}(e^2)}_{\text{LO, tree}} + \left[ \underbrace{\mathcal{O}\left(e^2 \frac{p^2}{16\pi^2 v^2}\right)}_{\text{NLO, 1-loop}} + \underbrace{\mathcal{O}\left(e^2 \frac{a_i p^2}{v^2}\right)}_{\text{NLO, tree}} \right], \quad (6)$$

<sup>1</sup> Other representations have been recently studied in Ref. [18].

	ECLh	ECL (Higgsless)
$\Gamma_{a_1-a_2+a_3}$	0	0
$\Gamma_{c_\gamma}$	0	-
$\Gamma_{a_1}$	$-\frac{1}{6}(1-a^2)$	$-\frac{1}{6}$
$\Gamma_{a_2-a_3}$	$-\frac{1}{6}(1-a^2)$	$-\frac{1}{6}$
$\Gamma_{a_4}$	$\frac{1}{6}(1-a^2)^2$	$\frac{1}{6}$
$\Gamma_{a_5}$	$\frac{1}{8}(b-a^2)^2 + \frac{1}{12}(1-a^2)^2$	$\frac{1}{12}$

**Table 1.** Running  $\frac{da_i^r}{d \ln \mu} = -\frac{\Gamma_{a_i}}{16\pi^2}$  of the relevant ECLh parameters and their combinations appearing in the six selected observables. The third column provides the corresponding running for the Higgsless EW chiral Lagrangian (ECL) case [4]. For the sake of completeness, we have added the running of the ECLh parameters  $a_4^r$  and  $a_5^r$ , which has been recently determined in the one-loop analysis of  $WW$ -scattering within the framework of chiral Lagrangians [7]. One can see that in the SM limit ( $a = b = 1$ ) these  $\mathcal{L}_4$  coefficients do not run, in agreement with the fact that these higher order operators are absent in the SM.

where  $e \sim \mathcal{O}(p/v)$  and  $A$  and  $B$  are given up to NLO by [5]

$$\begin{aligned}
A(\gamma\gamma \rightarrow zz)_{\text{LO}} &= B(\gamma\gamma \rightarrow zz)_{\text{LO}} = 0, \\
A(\gamma\gamma \rightarrow zz)_{\text{NLO}} &= \frac{2ac_\gamma^r}{v^2} + \frac{(a^2-1)}{4\pi^2 v^2}, & B(\gamma\gamma \rightarrow zz)_{\text{NLO}} &= 0, \\
A(\gamma\gamma \rightarrow w^+w^-)_{\text{LO}} &= 2sB(\gamma\gamma \rightarrow w^+w^-)_{\text{LO}} = -\frac{1}{t} - \frac{1}{u}, \\
A(\gamma\gamma \rightarrow w^+w^-)_{\text{NLO}} &= \frac{2ac_\gamma^r}{v^2} + \frac{(a^2-1)}{8\pi^2 v^2} + \frac{8(a_1^r - a_2^r + a_3^r)}{v^2}, & B(\gamma\gamma \rightarrow w^+w^-)_{\text{NLO}} &= 0.
\end{aligned} \tag{7}$$

The term with  $c_\gamma^r$  comes from the Higgs tree-level exchange in the  $s$ -channel, the term proportional to  $(a^2-1)$  comes from the one-loop diagrams with  $\mathcal{L}_2$  vertices, and the Higgsless operators in Eq. (5) yield the tree-level contribution to  $\gamma\gamma \rightarrow w^+w^-$  proportional to  $(a_1 - a_2 + a_3)$ . Independent diagrams are in general UV divergent. However, in dimensional regularization, the final one-loop amplitude turns out to be UV finite and one has  $a_1^r - a_2^r + a_3^r = a_1 - a_2 + a_3$ ,  $c_\gamma^r = c_\gamma$  [5], as in the Higgsless case [19].

In order to pin down each of the relevant combinations of ECLh couplings in Eq. (7) ( $a$ ,  $c_\gamma^r$  and  $a_1^r - a_2^r + a_3^r$ ) one must combine our  $\gamma\gamma$ -scattering analysis with other observables that depend on this same set of parameters. It is not difficult to find that other processes involving photons depend on these parameters. In Ref. [5] we computed 4 more observables of this kind: the  $h \rightarrow \gamma\gamma$  decay width (depending on  $a$  and  $c_\gamma$ ), the oblique  $S$ -parameter (depending on  $a$  and  $a_1$ ), and the  $\gamma^* \rightarrow w^+w^-$  (depending on  $a$  and  $a_2 - a_3$ ) and  $\gamma^*\gamma \rightarrow h$  (depending on  $c_\gamma$ ) electromagnetic form-factors. The one-loop contribution in these six relevant amplitudes is found to be UV-divergent in some cases. These divergences are absorbed by means of the generic  $\mathcal{O}(p^4)$  renormalizations  $a_i^r(\mu) = a_i + \delta a_i$ . As expected, the renormalization in the six observables gives a fully consistent set of renormalization conditions and fixes the running of the renormalized couplings in the way given in Table 1.

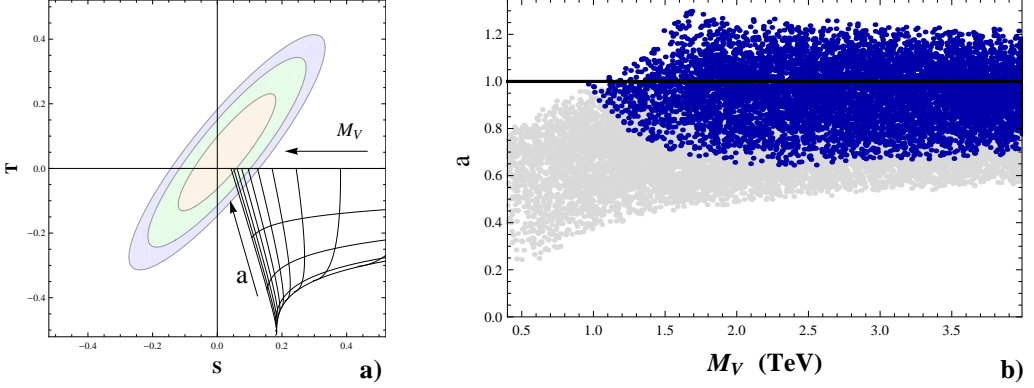


**Figure 1.** **a)** NLO determinations of  $S$  and  $T$ , imposing the two WSRs. The approximately vertical curves correspond to constant values of  $M_V$ , from 1.5 to 6.0 TeV at intervals of 0.5 TeV. The approximately horizontal curves have constant values of  $a$ : 0.00, 0.25, 0.50, 0.75, 1.00. The arrows indicate the directions of growing  $M_V$  and  $a$ . The ellipses give the experimentally allowed regions at 68% (orange), 95% (green) and 99% (blue) confidence level (CL). **b)** Scatter plot for the 68% CL region, in the case when only the first WSR is assumed. The dark blue and light gray regions correspond, respectively, to  $0.2 < M_V/M_A < 1$  and  $0.02 < M_V/M_A < 0.2$ .

### 3 Impact of spin-1 composite resonances on the oblique parameters

One can extend the range of validity and predictability of the ECLh by adding possible new states to the theory. Thus, the lightest V and A resonances are added to the EW Lagrangian in Ref. [14] in order to describe the oblique parameters  $S$  and  $T$  [9]. The relevant EW chiral invariant Lagrangian is given by the kinetic and Yang-Mills terms and the interactions [14]<sup>2, 3</sup>

$$\begin{aligned} \mathcal{L} = & \frac{v^2}{4} \langle u_\mu u^\mu \rangle \left( 1 + \frac{2a}{v} h \right) + \frac{F_V}{2\sqrt{2}} \langle V_{\mu\nu} f_+^{\mu\nu} \rangle + \frac{iG_V}{2\sqrt{2}} \langle V_{\mu\nu} [u^\mu, u^\nu] \rangle \\ & + \frac{F_A}{2\sqrt{2}} \langle A_{\mu\nu} f_-^{\mu\nu} \rangle + \sqrt{2} \lambda_1^{hA} \partial_\mu h \langle A^{\mu\nu} u_\nu \rangle. \end{aligned} \quad (8)$$

In order to compute  $S$  and  $T$  up to the one-loop level we use the dispersive representations [9, 14],

$$S = \frac{16\pi}{g^2 \tan \theta_W} \int_0^\infty \frac{dt}{t} [\rho_S(t) - \rho_S(t)^{\text{SM}}], \quad T = \frac{4\pi}{g'^2 \cos^2 \theta_W} \int_0^\infty \frac{dt}{t^2} [\rho_T(t) - \rho_T(t)^{\text{SM}}], \quad (9)$$

with  $\rho_S(t)$  the spectral function of the  $W^3 B$  correlator [9, 21] and  $\rho_T(t)$  the spectral function of the difference of the neutral and charged Goldstone self-energies [14]. The calculation of  $T$  above has been simplified by means of the Ward-Takahashi relation  $T = Z^{(w^+)} / Z^{(w^0)} - 1$  [20]. Only the lightest two-particle cuts have been considered in  $\rho_S(t)$  and  $\rho_T(t)$ , respectively,  $\{w\bar{w}, w\bar{h}\}$  and  $\{B\bar{w}, B\bar{h}\}$ . Since  $\rho_S(t)^{\text{SM}} \xrightarrow{t \rightarrow \infty} 0$ , the convergence of the Peskin-Takeuchi sum-rule requires  $\rho_S(t) \xrightarrow{t \rightarrow \infty} 0$ . Furthermore, assuming that weak isospin and parity are good symmetries of the BSM strong dynamics, the  $W^3 B$  correlator is proportional to the difference of the vector and axial-vector two-point Green's functions [9]. In asymptotically-free gauge theories this difference vanishes at  $s \rightarrow \infty$  as  $1/s^3$  [12], implying the (tree-level) LO WSRs [13],

$$F_V^2 - F_A^2 = v^2 \quad (\text{1st WSR}), \quad F_V^2 M_V^2 - F_A^2 M_A^2 = 0 \quad (\text{2nd WSR}). \quad (10)$$

<sup>2</sup> Here we follow the notation  $f_\pm^{\mu\nu} = u^\dagger \hat{W}^{\mu\nu} u \pm u \hat{B}^{\mu\nu} u^\dagger$  from Ref. [14, 21], where there is a global sign difference with [5] in the definitions of  $\hat{W}_\mu$  and  $\hat{B}_\mu$ . The spin-1 resonances are described in the antisymmetric tensor formalism [8].

<sup>3</sup> In other works, the coupling  $a$  can be found with the notation  $\kappa_W$  and  $\omega$  [14] or  $\kappa_V$  [22].

	$a$	$M_V$
two WSRs	$0.97 - 1$	$> 5 \text{ TeV}$
Only 1st WSR: $0.2 < M_V/M_A < 1$	$0.6 - 1.3$	$> 1 \text{ TeV}$
$0.5 < M_V/M_A < 1$	$0.84 - 1.30$	$> 1.5 \text{ TeV}$
$M_V/M_A = 1$	$0.97 - 1.30$	$> 1.8 \text{ TeV}$
$(M_V > 1 \text{ TeV})^\dagger \quad 1 < M_V/M_A < 2$	$0.7 - 1.9$	$> 1 \text{ TeV}^\dagger$

**Table 2.** Allowed range for the  $M_V$  and  $a$  at the 68% CL for the two-WSRs (where  $V$  and  $A$  are very degenerate since  $M_V^2/M_A^2 = a$  in this case) and only-1st-WSR cases (for various values  $M_V/M_A$ ). In the last line we also impose the restriction<sup>†</sup>  $M_V > 1 \text{ TeV}$ .

However, although the 1st WSR is expected to be true in gauge theories with non-trivial ultraviolet fixed points [10, 11], the 2nd WSR is questionable in some of these models. Thus, two alternative scenarios are studied in Ref. [14]: one assuming the two WSRs and another assuming just the 1st WSR. At tree-level one has the LO determinations [9, 14, 21]

$$S_{\text{LO}} = 4\pi \left( \frac{F_V^2}{M_V^2} - \frac{F_A^2}{M_A^2} \right) = \frac{4\pi v^2}{M_V^2} \left( 1 + \frac{M_V^2}{M_A^2} \right) \quad (\text{1st \& 2nd WSR}), \quad (11)$$

$$S_{\text{LO}} = 4\pi \left\{ \frac{v^2}{M_V^2} + F_A^2 \left( \frac{1}{M_V^2} - \frac{1}{M_A^2} \right) \right\} > \frac{4\pi v^2}{M_V^2} \quad (\text{1st WSR \& } M_V < M_A).$$

In the first case, the two WSRs imply  $M_V < M_A$  and determine  $F_V$  and  $F_A$  in terms of the resonance masses [8, 9, 14, 21]. In the second case, it is not possible to extract a definite prediction with just the 1st WSR but one can still derive the inequality above if one assumes a similar mass hierarchy  $M_V < M_A$ . On the other hand, this inequality flips direction if  $M_A < M_V$  or turns into an equality in the degenerate case  $M_V = M_A$  [14]. At NLO the computed  $W^3B$  correlator is given by the  $ww$  and  $hw$  cuts, whose contributions to the  $\rho_S(t)$  spectral function would have an unphysical grow at high energies unless  $F_V G_V = v^2$  and  $F_A \lambda_1^{hA} = av$  [8, 14, 21]. Thus, we obtain the NLO prediction [14]

$$S = 4\pi v^2 \left( \frac{1}{M_V^2} + \frac{1}{M_A^2} \right) \quad (12)$$

$$+ \frac{1}{12\pi} \left[ \log \frac{M_V^2}{m_H^2} - \frac{11}{6} + \frac{M_V^2}{M_A^2} \log \frac{M_A^2}{M_V^2} - \frac{M_V^4}{M_A^4} \left( \log \frac{M_A^2}{m_{S_1}^2} - \frac{11}{6} \right) \right] \quad (\text{1st \& 2nd WSR}),$$

$$S > \frac{4\pi v^2}{M_V^2} + \frac{1}{12\pi} \left[ \log \frac{M_V^2}{m_H^2} - \frac{11}{6} - a^2 \left( \log \frac{M_A^2}{m_{S_1}^2} - \frac{17}{6} + \frac{M_A^2}{M_V^2} \right) \right], \quad (\text{1st WSR \& } M_V < M_A).$$

In the two-WSRs scenario, in order to enforce the 2nd WSR at NLO one needs the additional constraint  $a = M_V^2/M_A^2$  (hence restricted to the range  $0 \leq a \leq 1$ ). Again, the inequality in the last line flips direction or turns into an equality when, respectively,  $M_A < M_V$  or  $M_V = M_A$ .

At LO,  $\rho_T(t)$  is zero and one has  $T_{\text{LO}} = 0$ . At NLO, where we enforce the  $\rho_S(t)$  constraints  $F_V G_V = v^2$  and  $F_A \lambda_1^{hA} = av$ , we find that  $\rho_T(t) \xrightarrow{t \rightarrow \infty} 0$  and obtain the NLO prediction

$$T = \frac{3}{16\pi \cos^2 \theta_W} \left[ 1 + \log \frac{m_h^2}{M_V^2} - a^2 \left( 1 + \log \frac{m_h^2}{M_A^2} \right) \right], \quad (13)$$

In Fig. 1, we show the compatibility between the experimental determinations for  $S$  and  $T$  [15] and our NLO determinations in both scenarios. The numerical results in Table 2 show that the precision

electroweak data requires resonance masses over the TeV and the  $hWW$  coupling to be close to the SM one ( $a^{\text{SM}} = 1$ ), in agreement with present LHC bounds [22].

To conclude, we emphasize that, remarkably, just by considering the experimental  $m_h$  (the only LHC input) and the EW precision observables (LEP input), the allowed region concentrates around  $a \simeq 1$  for reasonable values of the splitting  $M_V/M_A \sim \mathcal{O}(1)$  (see Fig. 1 and Table 2).

## References

- [1] S. Weinberg, *Physica* **A96** (1979) 327; J. Gasser and H. Leutwyler, *Annals Phys.* **158** (1984) 142; *Nucl. Phys. B* **250** (1985) 465; *Nucl. Phys. B* **250** (1985) 517.
- [2] T. Appelquist and C. W. Bernard, *Phys. Rev. D* **22** (1980) 200.
- [3] A. C. Longhitano, *Phys. Rev. D* **22** (1980) 1166; *Nucl. Phys. B* **188** (1981) 118.
- [4] Maria J. Herrero and Ester Ruiz Morales, *Nucl.Phys. B* **418** (1994) 431.
- [5] R.L. Delgado, A. Dobado, M.J. Herrero, J.J. Sanz-Cillero, *JHEP* **1407** (2014) 149.
- [6] J. Hirn and J. Stern, *Phys.Rev. D* **73** (2006) 056001; G. Buchalla and O. Catà, *JHEP* **1207** (2012) 101.
- [7] D. Espriu and B. Yenko, *Phys. Rev D* **87** (2013) 055017; D. Espriu, F. Mescia and B. Yenko, *Phys. Rev D* **88** (2013) 055002; D. Espriu and B. Mescia, *Phys.Rev. D* **90** (2014) 015035; R. L. Delgado, A. Dobado, F. J. Llanes-Estrada, *J.Phys. G* **41** (2014) 025002; *JHEP* **1402** (2014) 121.
- [8] G. Ecker *et al.*, *Nucl. Phys. B* **321** (1989) 311; G. Ecker *et al.*, *Phys. Lett. B* **223** (1989) 425.
- [9] M. E. Peskin and T. Takeuchi, *Phys. Rev. D* **46** (1992) 381; *Phys. Rev. Lett.* **65** (1990) 964.
- [10] A. Orgogozo and S. Rychkov, *JHEP* **1203** (2012) 046.
- [11] T. Appelquist and F. Sannino, *Phys. Rev. D* **59** (1999) 067702.
- [12] C. W. Bernard, A. Duncan, J. LoSecco and S. Weinberg, *Phys. Rev. D* **12** (1975) 792.
- [13] S. Weinberg, *Phys. Rev. Lett.* **18** (1967) 507.
- [14] A. Pich, I. Rosell and J.J. Sanz-Cillero, *Phys.Rev.Lett.* **110** (2013) 181801; *JHEP* **1401** (2014) 157.
- [15] M. Baak *et al.*, *Eur. Phys. J. C* **72** (2012) 2205; <http://gfitter.desy.de/>; LEP Electroweak Working Group, <http://lepewwg.web.cern.ch/LEPEWWG/>.
- [16] S. Matsuzaki *et al.*, *Phys. Rev. D* **75** (2007) 073002; R. Barbieri *et al.*, *Phys. Rev. D* **78** (2008) 036012; O. Catà and J.F. Kamenik, *Phys. Rev. D* **83** (2011) 053010; A. Orgogozo and S. Rychkov, *JHEP* **1306** (2013) 014.
- [17] J. M. Cornwall, D. N. Levin and G. Tiktopoulos, *Phys.Rev. D* **10** (1974) 1145, Erratum-ibid. **D 11** (1975) 972; C.E. Vayonakis, *Lett.Nuovo Cim.* **17** (1976) 383; B.W. Lee, C. Quigg and H.B. Thacker, *Phys.Rev. D* **16** (1977) 1519; G.J. Gounaris, R. Kogerler and H. Neufeld, *Phys.Rev. D* **34** (1986) 3257.
- [18] M.B. Gavela, K. Kanshin, P.A.N. Machado and S. Saa, [arXiv:1409.1571 [hep-ph]].
- [19] M. J. Herrero and E. Ruiz-Morales, *Phys.Lett. B* **296** (1992) 397; J. Bijnens and F. Cornet, *Nucl. Phys. B* **296** (1988) 557; J. F. Donoghue, B. R. Holstein and Y.C. Lin, *Phys.Rev. D* **37** (1988) 2423; J. Bijnens, S. Dawson and G. Valencia, *Phys. Rev. D* **44** (1991) 3555.
- [20] R. Barbieri *et al.*, *Nucl. Phys. B* **409** (1993) 105.
- [21] A. Pich, I. Rosell and J.J. Sanz-Cillero, *JHEP* **1208** (2012) 106.
- [22] ATLAS Collaboration, Report No. ATLAS-CONF-2014-009; CMS Collaboration, Report No. CMS-PAS-HIG-14-009.